An Accurate Groove Position Detection Using Soft-Focused Imaging†

Katsunori INOUE*, Mamoru KAWAHARA** and Yoshiaki ARATA***

Abstract

This paper discussed a visudal seam tracking control method, in which a light sectioning technique by laser and image sensor is used for imaging the sectional pattern of joint groove and a microcomputer is used for image processing and producing the control output. The image processing method used here is applicable to various shapes of joint groove, and even effective for the presence of previous weld passes. Another feature of this method is that the picture pickup optical system is intentionally put out of focus; by processing this out-of-focus image, the detection resolution better than that determined from the number of image sensor elements has been successfully achieved. An automatic seam tracking controller based on this method has been applied to a large-diameter steel pipe production line, proving that it is practical and useful, and contributes to improvement of the weld quality.

KEY WORDS: (Automatic Welding) (Seam Tracking) (Image Processing) (Pattern Recognition) (Sensor) (Computer)

1. Introduction

This paper describes a new image processing method to detect welding groove for a seam tracking sensor. Especially emphasizing point is placed on a higher accurate groove position detection method by using a soft focused groove image.

Recently, there is a trend toward the use of visual sensors in the field of automatic control equipment, industrial robots, etc. to overcome difficulties in automation and to achieve a higher degree of automation[1]. When taking an image by CCD camera, or when processing an image using computer, these pictures are essentially digitalized. A digital image has resolution limit determined by the number of image elements (pixels) of which the image is composed. When improvement of detection accuracy is needed in the field of image processing technology, it is usually necessary to increase the number of pixels. But if the number of pixels is increased, it leads to an increase of processing time as a matter of course. On the other hand, there is a strong demand to reduce an image processing time as short as possible. Therefore it is greatly necessary to balance detection accuracy and image processing time.

Figure 1 shows the principle of groove shape pattern determination by the light-sectioning technique[2]. This visual sensor hardware consists of a laser beam projector and a CCD camera. The projector fans out a flat beam of light to irradiate the welding groove slantwise from above and at right angles to the weld line. When viewed from directly above the groove, this bright line describes the cross-section of the groove and is taken by the camera as the image of the groove.

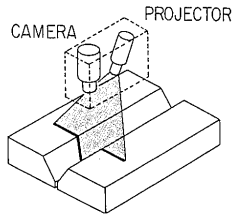

Fig. 1 Principle of image detection.

In this paper, a new image processing method is discussed. Keeping an adequate detection accuracy, the method can reduce processing time. The method discussed here is unique in using an image which consists of a considerably small number of pixels for reducing processing time, and in using the out-of-focus imaging intentionally. This method has achieved a higher resolution than that determined from the number of pixels by processing the out-of-focus image.

An automatic seam tracking controller based on this method has been tested and applied to a large diameter steel pipe production line, proving that it is practical and useful, and contributes to improvement of the weld quality and work efficiency.

The discussion is made in four sections and in the following order: effect of out-of-focus imaging, image

† Received on May 8, 1989
* Professor
** Kansai Tech Co.
*** Emeritus Professor

Transactions of JWRI is published by Welding Research Institute of Osaka University, Ibaraki, Osaka 567, Japan

processing software, experimental results and an application to steel pipe production.

2. Effect of Out-of-Focus Imaging

In this section, it is discussed why higher detection accuracy is achieved by using an out-of-focus image. To simplify the discussion, detection of a single side edge is condidered. **Figure 2** shows an illustrated picture of a

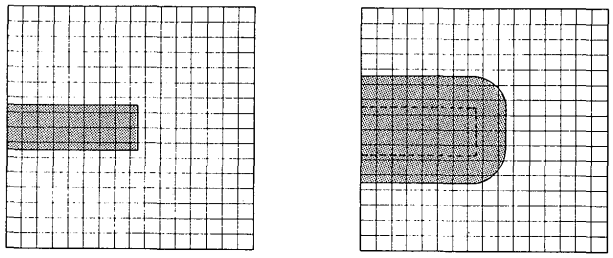

(a) (b)

Fig. 2 Illustrated images for discussion.

single side edge taken by a camera. **Figure 2(a)** shows an in-focus image and (b) shows an out-of -focus image. Cross points of a lattice show elements of an image sensor. In the case of Fig. 2(a), band width consists of three pixels. If the object moves to the right, three pixels which indicate a right edge move intermittently one pixel distance all at once to the right. In other words, pixel condition of the image does not change during the object moves some distance which corresponds to one pixel distance on the screen. In the case of **Fig. 2(b)**, the image is out-of-focused, then band width consists of seven pixels and a right edge of the image is roundish. In this case, when the obejct moves to the right, seven pixels which form a right edge portion move one pixel distance to the right independently, not simultaneously. That is to say, during the object moves one pixel corresponding distance, pixel condition of the image changes separately several times.

Figure 3 shows an close-up view of an edge portion. The picture co-ordinate system is an follows: the upper

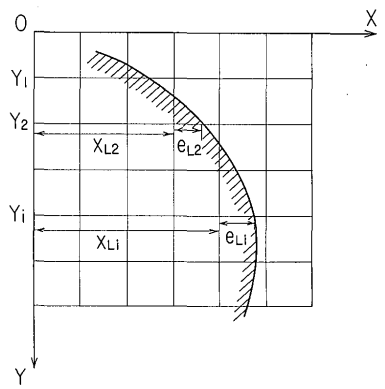

Fig. 3 Edge part of the image for discussion.

left-hand corner of the picture area is the origin (0), from which X-axis extends horizontally to the right and Y-axis extends vertically downward.

We let $Y_1, Y_2, \ldots\ldots, Y_k$ be a Y-axis value of an image, respectively, then right edge positions on X-axis are calculated in **Eq. (1)** as follows:

$$X = X_{Li} + e_{Li} \ (i = 1, 2, \ldots\ldots, k) \tag{1}$$

where X_{Li} is integer which counts pixel unit, and the right edge position is observed at $X = X_{Li}$ because of a digital picture characteristic in spite of the true right edge being $X_{Li} + e_{Li}$. The e_{Li} is a quantization error with $0 \leqslant e_{Li} < 1$. The minimum value among k quantization errors e_{Li} s' is calculated, and subtract the minimum value from each e_{Li}, and these calculated values are arranged in order of smaller value, then a new permutation,

$$e_1', e_2', e_3', \ldots\ldots, e_k'$$

is obtained. If the object moves to the right, and let X be an image displacement on the screen, pixel condition is changed at $X = e_1'$, $X = e_2'$, ..., $X = e_k'$, respectively, during the image moves one pixel to the right.

Under above mentioned circumstances, we define the detection error, e_{max}, as the longest interval in which no change of pixel condition happens. Then the detection error, e_{max}, is calculated as follows in **Eq. (2)**:

$$e_{max} = \max (\ e_i' - e_{i+1}' \ ; i = 1, 2, 3, \ldots\ldots, k) \tag{2}$$

where $e_1' \leqslant e_{i+1}'$, $e_1' = 0$, $e_{k+1}' = 1$. **Equation (2)** indicates that the detection error e_{max} is the maximum absolute difference of neighbouring two values, $e_i' - e_{i+1}'$, among k quantization errors.

In the case, of Fig. 2 (a), $e_1' = e_2' = e_3' = 0$ and $e_4' = 1$, then $e_{max} = 1$ (pixel).

At a second stage of our consideration, a result of simulation study is discussed. In this paragraph, every grade of out-of-focus imaging is simulated, and e_{max} in Eq.(2) is calculated for every image. At first, a producing method of an out-of-focus image is mentioned. We let (ξ, η) and (X, Y) be a co-ordinates of an object plane and an image plane, respectively. An out-of-focus image V(X, Y) is calculated according to the following equation[3].

$$V(X, Y) = \int_{-\infty}^{\infty}\int_{-\infty}^{\infty} v(\xi, \eta)\, h(X-\xi, Y-\eta)\, d\xi\, d\eta \tag{3}$$

where $v(\xi, \eta)$ is a geometrical distribution of an object and h(X, Y) is the point spread function of the supposing out-of-focus imaging optical system.

If this imaging system has a circular aperture, and if an approximation theory of geometrical optics can be

applied, the point spread function h(X, Y) is assumed as a following cylindrical function with radius R(in **Eq. 4**).

$$h(X, Y) = \begin{cases} \dfrac{1}{\pi R^2} & ;\sqrt{x^2+Y^2} \leqslant R \\ 0 & ;\sqrt{x^2+Y^2} > R \end{cases} \quad (4)$$

where radius R is related to the degree of out-of-focus imaging.

Figure 4 shows an simulation result on detection error e_{max} for every R. In this simulation, V(X, Y) is calculated using Eq.(3), a binary image is produced with a threshold level which is 50 percent of the maximum brightness level of V(X, Y), and e_{max} is evaluated using Eq.(2). The horizontal axis indicates R, and the vertical axis indicates an edge width k, detection error e_{max} and a relative brightness level. Figure 4 shows that higher the degree of out-of-focus imaging, smaller the detection error e_{max}. But at the same time, we can see that higher the degree, lower the brightness level of the image. Therefore if we put the degree of out-of-focus imaging high, the detection error e_{max} becomes small theoretically, but brightness level becomes also low and the S/N ratio becomes low, then there is a lower limit of e_{max} because of noisy imaging. There must be the optimum level of R, and in our simulation study, it is near to optimum at from R = 3 to R = 4. In the optimum state of R, e_{max} is nearly equal to 0.5 (pixel), the brightness level is 50 percent of that of R = 0, and the edge width k is twice as large as that of R = 0.

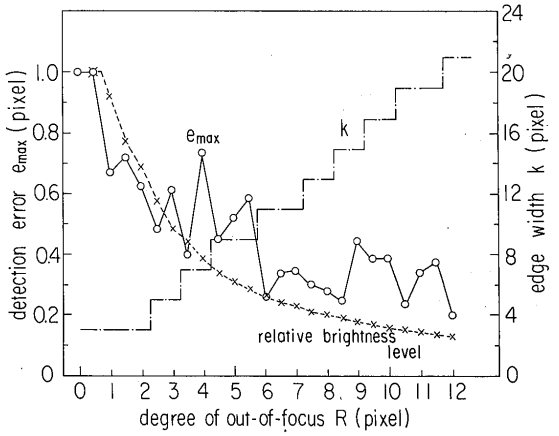

Fig. 4 Simulation result on detection error.

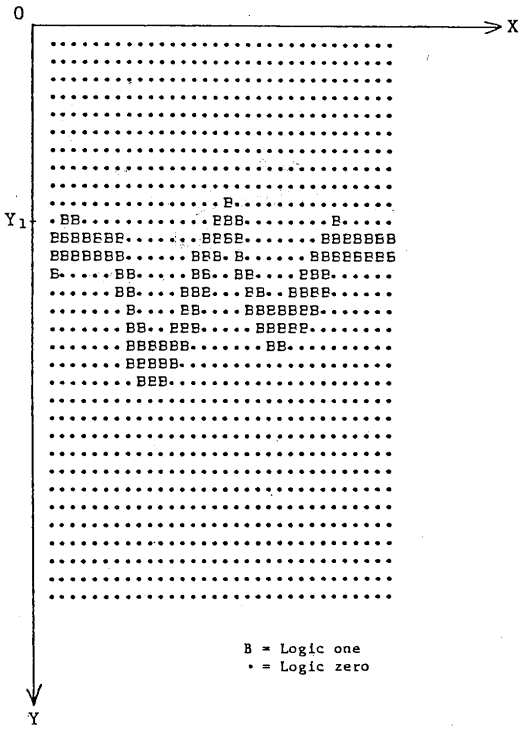

Fig. 5 Image data matrix.

3. Image Processing Software

3.1 Pattern screening and compression

The pattern screening and compression are processed to remove non-essential data from the image data matrix and to reduce it to an essential set of data for simplification of later processing, i.e., groove center position computation. **Figure 5** shows an example of image data matrix. For each row of the image data matrix, the number, n_d, of data pixels (image matrix elements that are in Logic One state, receiving the laser light reflected from the joint) is counted, starting from the first row (Y = 1) and on. As understood from Fig. 5, the surface of steel plates can be recognized from several consecutive rows of n_d sufficiently greater than zero, and the other rows are non-essential. Therefore, as n_d counting proceeds from the first row, second row and so on, the row that first shows the inequality $n_d \geqslant \delta$ (y = judgment parameter) is judged to be the start of steel surface portion data. In Fig. 5, the row of $Y = Y_1$ corresponds to this. The rows from this on are picked up as significant data until a row that does not satisfy the inequality $n_d \geqslant \delta$ is found, i.e., rows of $Y = Y_1, Y_2, Y_3, \ldots, Y_k$ ($n_d < \delta$ for $Y = Y_{k+1}$) are picked up, or until k reaches k_{max}.

The k rows of steel surface data as screened above are then OR-operated on each column and compressed into a single row of data.

3.2 Pattern classification

Considering the varying factors, such as the groove shape, presence of bead and base metal surface conditions, the image data compressed into a single row is assumed to take one of eight basic patterns:

(i) D_1, B_2, D_2
(ii) B_1, D_1, B_2, D_2
(iii) D_1, B_2, D_2, B_3

(iv) B_1, D_1, B_2, D_2, B_3
(v) D_1, B_2, D_2, B_3, D_3
(vi) $B_1, D_1, B_2, D_2, B_3, D_3$
(vii) $D_1, B_2, D_2, B_3, D_3, B_4$
(viii) $B_1, D_1, B_2, D_2, B_3, D_3, B_4$

where:

B_1 = number of consecutive Blank (Logic Zero) pixels as counted from the most left of the row;
D_1 = number of consecutive Data (Logic One) pixels as counted from the most left of the row, or which follow B_1;
B_2 = number of consecutive Blank pixels following D_1;
D_2 = number of consecutive Data pixels following B_2;
B_3 = number of consecutive Blank pixels following D_2;
D_3 = number of consecutive Data pixels following B_3;
B_4 = number of consecutive Blank pixels following D_3;

Among these basic patterns, pattern (i) represents basically the narrow groove joint with D_1 and D_2 being the base metal surfaces and B_2 being the groove. Patterns (ii) through (viii) are variations of pattern (i) with loss of data piexels at the right or left end of the row, bead height in the groove, and others. If the sensed image pattern does not agree with any of these basic patterns, then the data will be ignored as abnormal and not processed.

3.3 Computation of groove center position

The left and right groove edge positions are determined in terms of the number of pixels as counted from the most left of the picture (X-axis), then the median value between them is computed as the groove center position.

First, the left and right edge positions, X_L and X_R, are determined from the compressed image data as **Fig. 5.**

For pattern (i) or (iii) :

$$X_L = D_1$$
$$X_R = D_1 + B_2 + 1$$

For pattern (ii) or (iv) :

$$X_L = B_1 + D_1$$
$$X_R = B_1 + D_1 + B_2 + 1$$

For pattern (v) or (vii) :

$$X_L = D_1$$
$$X_R = D_1 + B_2 + D_2 + B_3 + 1$$

For pattern (vi) or (viii) :

$$X_L = B_1 + D_1$$
$$X_R = B_1 + D_1 + B_2 + D_2 + B_3 + 1 \qquad (5)$$

Next, for each of the k rows of joint surface data screened as mentioned in Section 3.1, the left and right edge positions, X_{Li} and X_{Ri}, are determined according to **Eq. 6.**

$$X_{Li} = \max \{ X \mid V(X, Y_i) = 1, X_L - d < X < X_L \}$$
$$X_{Ri} = \min \{ X \mid V(X, Y_i) = 1, X_R < X < X_R + d \}$$
$$i = 1, 2, \ldots\ldots, k \qquad (6)$$

where V(X, Y) represents the logic level (Logic Zero or One) of an element at position (X, Y) of the binary image, and d is the parameter to define the permissible range of spread of X_{Li}, X_{Ri}. From the edge position data (X_{Li}) and (X_{Ri}) obtained using Eq. (6), the groove center position is computed according to:

$$X_0 = \frac{1}{2k_L} \sum_{i=1}^{k_L} X_{Li} + \frac{1}{2k_R} \sum_{i=1}^{k_R} X_{Ri} \qquad (7)$$
$$k_L, k_R \leqslant k$$

Equation (7) means to compute the arithmetic mean $\overline{X_L}$ and $\overline{X_R}$ of ($\overline{X_{Li}}$) and ($\overline{X_{Ri}}$), respectively, then to compute the median value between $\overline{X_L}$ and $\overline{X_R}$. The number of data operated on, k_L for the left edge and k_R for the right edge, may not agree with the number of rows, k, picked up in the screening process, but may be smaller than k with some data rejected as being out of range in Eq. (6) computation process.

The X_0 value as obtained in various conventional image processing methods is equivalent to computing it as $(X_L + X_R)/2$ from X_L and X_R calculated using Eq. (5). Comparison of X_0 values according to Eq. (7) with conventional X_0 values is discussed in Section 4.

4. Experimental Results on Groove Center Detection Accuracy

The method used here to determine the accuracy of the groove center detection is as follows. A joint groove test piece is placed on a precision slide table, so that the groove position can be changed in directions perpendicular to the weld line. For values of the groove position displacement x (mm) from the assumed center position (x = 0 mm), the image sensing and processing equipment computes the groove center position X_0. They should hold a linear relationship between x and X_0, but no ideal linear relationship will be obtained due to quantization and image processing errors. Therefore, for a group of data (x, X_0), a straight regression line is fitted, and deviations of the individual X_0 values from this regression line are calculated to obtain a distribution of these deviations. Then the largest value among these deviations is defined as the detection error. The camera in this experiment has a two-dimensional solid-state image sensor with a pixel matrix of 32 X 32, the number of pixels supposed to be very small.

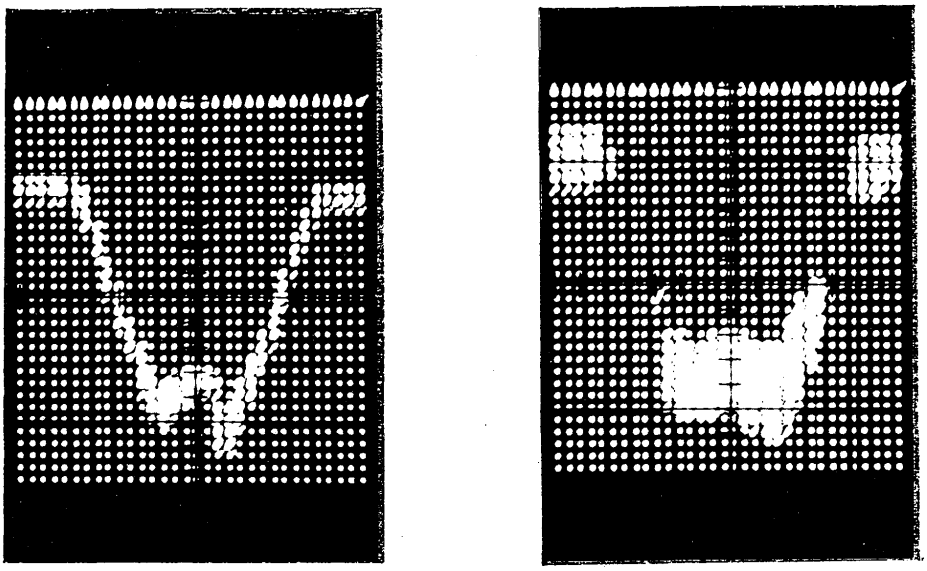

(a) In-focus image (b) Out-of-focus image

Fig. 6 Binary images of a tack weld joint groove.

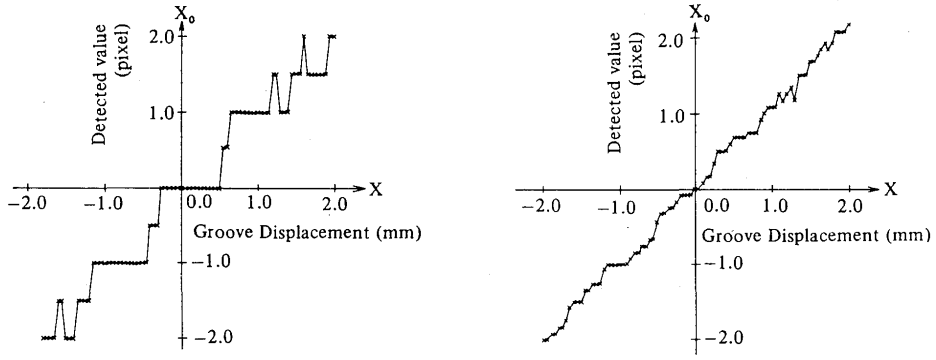

(a) In-focus imaging. (b) Out-of-focus imaging.

Fig. 7 Groove center detection results.

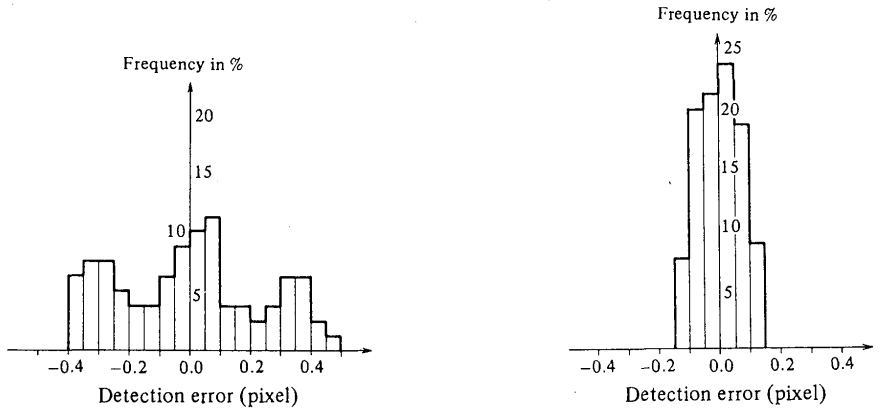

(a) In-focus imaging. (b) Out-of-focus imaging.

Fig. 8 Distribution of groove center detection error.

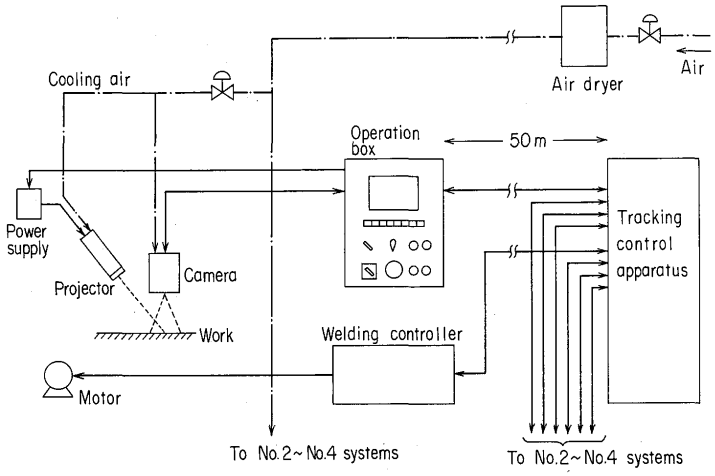

Fig. 9 Construction of an automatic tracking system using the visual sensor.

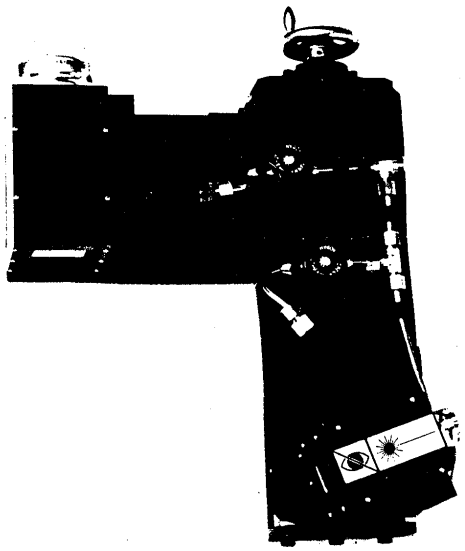

Fig. 10 Tracking sensor.

Figure 6 compares two binary images of the same groove obtained by processing the picture taken: (a) in-focus condition and (b) out-of-focus condition, indicating that the latter provides a much greater number of data pixels for groove center position computation.

Figure 7 shows the groove center detection results for two cases of imaging: (a) in-focus conditio and (b) out-of-focus condition. In case of (a), errors due to quantization of the picture to pixels by the image sensor are clearly seen. Whereas, in case of (b), nearly a straight-line relationship is seen, indicating that the out-of-focus imaging reduces the quantization errors and achieves a high accuracy in groove center detection.

Figure 8 shows a frequency distribution of X_0 deviations in pixels from the regression line, for Fig. 7 cases (a) and (b). The detection error is 0.50 pixel for case (a) in-focus imaging, and 0.15 pixel for case (b) out-of-focus imaging. From these results, it is clear that the out-of-focus imaging and processing much improves the detection accuracy.

5. An Application Example

The groove shape sensing and tracking control system discussed here has been applied to large-diameter steel pipe production lines. In the production line, thick steel plate is bent into a cylindrical shape; and the seam is welded from the inside first. Next, the same seam is welded from the outside. The steel pipe is further adjusted for final shape, checked and inspected, surface-treated and finished, then leaves the line as product. This tracking control system is applied to the outside welding process of the above steel pipe production line.

Figure 9 shows the seam tracking system for this application. This system consists of a laser beam projector, a solid-state camera, an operation box and a tracking controller. Signals for start and stop of seam tracking are sent from a welding controller, therefore no manual operation for seam tracking is necessary.

Figure 10 shows a photograph of the tracking sensor which consists of a laser beam projector and a camera.

Figure 11 shows a manual tracking result by a skilled operator. In this experiment, the automatic tracking system did not control the torch positioning, but carried out only groove position detection. The horizontal axis represents time duration and the first row of the vertical axis represents tracking error calculated by the system. One division of the vertical axis is equal to 0.17 pixel of an obtained image. The fourth row of the vertical axis represents an control output which might drive servo-mechanism if the system was in automatic mode.

Figure 12 shows an automatic tracking control result operated by the system. The first and fourth row of the

Fig. 11 An example of seam tracking result manually handled by a skilled operator.

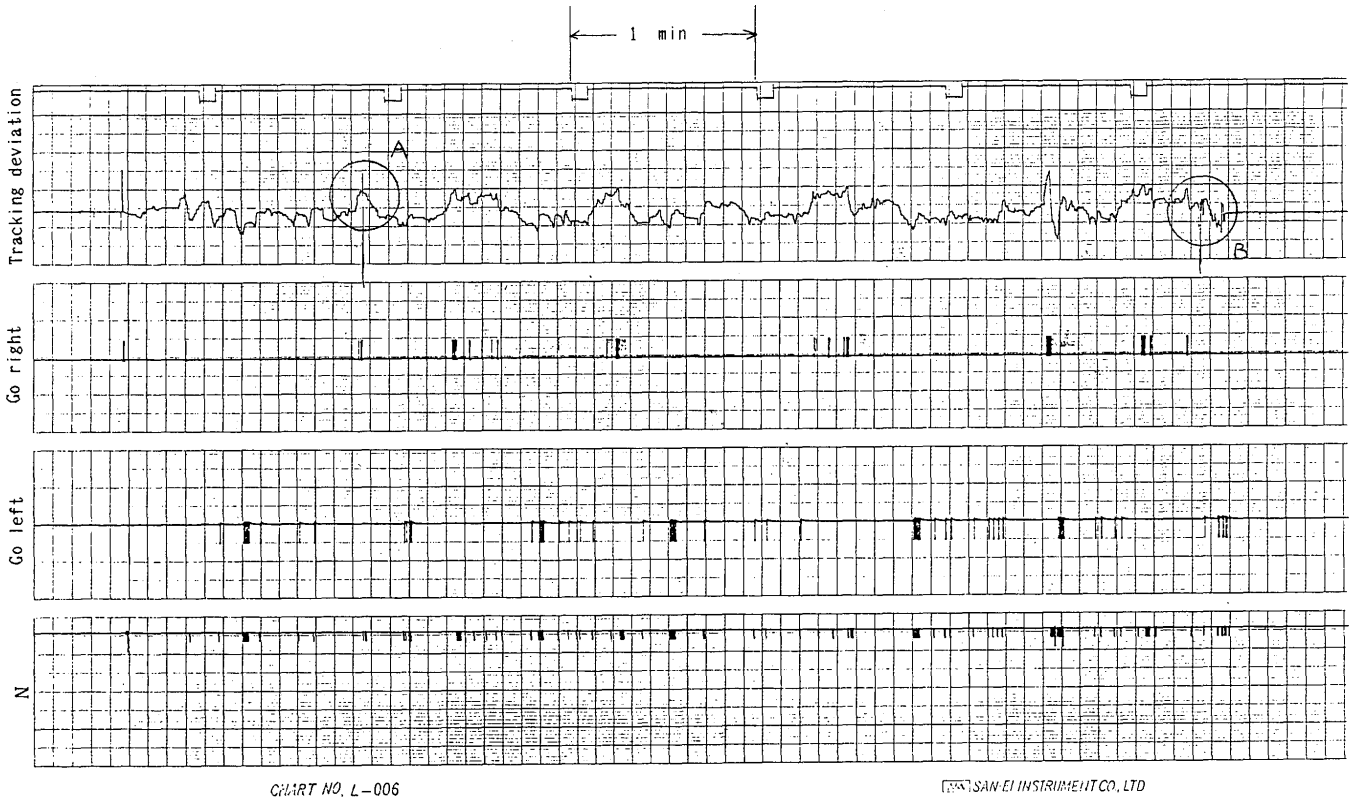

Fig. 12 An example of seam tracking result controlled by the visual tracking system.

vertical axis also indicate tracking error and control output, respectively. The second and third row of the vertical axis show moving directions of a servomechanism, right and left.

Comparing Figs. 11 and 12, tracking error of the automatic seam tracking system was restricted in narrower range than the manually controlled case. Then it is expected that weld quality has been improved. In Fig. 12, there can be seen a sudden change of tracking error at the points marked A and B. It is supposed that some unusual image caused this sudden change, and image processing program could safely recognize this abnormality and avoid miss control.

The tracking control system introduced this time has achieved the target control accuracy of 0.5 mm in automatic tracking, improving both weld quality and work efficiency.

6. Conclusion

The automatic seam tracking control system as developed and discussed in this paper uses a combination of laser and image sensor for groove profile detection and a microcomputer for image processing. The system is applicable to a variety of groove shapes, even to prebeaded joints, whose groove profile is complex and considered difficult to track. Also, by making the pickup optical system out of focus and processing the out-of-focus groove image, the error of the groove center position detection is reduced to 1/3 of that in in-focus imaging.

The system has been successfully applied to large diameter steel pipe production, improving both weld quality and work efficiency, and demonstrating its usefulness.

Acknowledgment

A part of this research work was done when one of the authors belonged to HITACHI ZOSEN CORPORATION. The authors would like to express their gratitude to engineers of the company who have been taking part in developing the control system.

References

1) Y. Arata and K. Inoue: Application of digital computer to pattern measurement and processing in automatic control system of welding, J. Jap. Welding Soc., Vol. 46 (1977), 129–134 (in Japanese).
2) M. Kawahara: Tracking Control System Using Image Sensor for Arc Welding, Automatica, Vol. 19 (1983), No. 4 357–363.
3) J. Maeda and K. Murata: Estimation of the Point Spread Function of a Defocussed System and Restoration of the Images, Kogaku, Vol. 7 (1978), No. 1, 12–20 (in Japanese).